Biosensors and Bioelectronics 141 (2019) 111209

Contents lists available at ScienceDirect

Biosensors and Bioelectronics

journal homepage: www.elsevier.com/locate/bios

# Disease antigens detection by silicon nanowires with the efficiency optimization of their antibodies on a chip

Dong-Sheng Su[a,b,1], Po-Yen Chen[a,c,1], Hsiang-Chih Chiu[d,*], Chien-Chung Han[c,*], Ta-Jen Yen[b,e,*], Hueih-Min Chen[a,*]

[a] National Applied Research Laboratories,Taiwan Semiconductor Research Institute, Hsinchu, Taiwan
[b] Department of Materials Science and Engineering, National Tsing Hua University, Hsinchu, Taiwan
[c] Department of Chemistry, National Tsing Hua University, Hsinchu, Taiwan
[d] Department of Physics, National Taiwan Normal University, Taipei, Taiwan
[e] Center for Nanotechnology, Materials Science, and Microsystems, National Tsing Hua University, Hsinchu, Taiwan

ARTICLE INFO

*Keywords:*
Antigen detection
Antibodies
Nanowires
Efficiency optimization of protein
EOP)

ABSTRACT

Enhancing the efficiency of antibody protein immobilized on a silicon nanowire-based chip for their antigens detection is reported. An external electric field (EEF) is applied to direct the orientation of antibodies during their immobilization on a chip. Atomic force microscopy (AFM) is used to measure the binding forces between immobilized antibody and targeting antigen under the influence of EEF at different angles. The maximum binding force under a specific angle (optimal angle; oa) of EEF ($_{max}EEF^{oa}$) implies the optimal orientation of the antibodies on the chip. In this report, two different cancer carcinoembryonic antigen (CEA)-related cell adhesion molecules 5 (CEACAM5) & 1 (CEACAM1) were used for the examples of disease antigen detection. $_{max}EEF^{oa}$ of anti-CEACAM5 or anti-CEACAM1 immobilized on a general chip was firstly determined. Spectroscopy of AFM revealed that both binding forces were the largest ones with their antigens when $_{max}EEF^{oa}$ was applied as compared with no or other angles of EEF. These antibody proteins accompanied with the application of EEF were secondly immobilized on silicon-nanowires (n = 1000) and the field effects were measured (ΔI) as their target antigens were approached. Results showed that ΔI was the largest ones when $_{max}EEF^{oa}$s (225°/270° and 135°/180° for anti-CEACAM5 and anti-CEACAM1, respectively) were applied as compared with other angles of EEF. These observations imply that the silicon nanowires together with the application of $_{max}EEF^{oa}$ as detection tools could be applied for the cancer diagnostics in the future.

## 1. Introduction

Disease detection and identification have been progressing in the past decades. Especially, both technologies of DNA sequencing (Al-Shereiqi et al., 2015; Bracha et al., 2014; Caruso et al., 1997) and protein chip (Rusmini et al., 2007) have accelerated the understanding about biomolecules both *in vivo* and *in vitro* (Dong et al., 2006; Sin et al., 2014; Wang et al., 2013; Xing et al., 2005). Early disease detection *via* general physical examinations for health consideration by using these technologies is always demanded. However, current detection techniques with limited accuracy and less efficiency may be a concern nowadays. For example, the popular clinical technique used for cancer detection is the enzyme-linked immuno-sorbent assay (ELISA) (Han et al., 2007; Seo et al., 2010). ELISA is mainly based on two antibodies forming an antibody-antigen-antibody type of "sandwich" (one of ELISA methods) with immobilized primary antibody and secondary antibody labeled with fluorescence dyes to bind with the antigen. The concentration of antigen can be calculated from the fluorescence intensity gained due to the quantity of secondary antibody bound with antigen. However, the detection accuracy is possibly limited by the inefficiency of the qualified binding between antibodies and target antigens since many immobilized primary antibodies are not in the right positions for the binding. Other detection techniques with various detection sources such as surface plasmon resonance (SPR) (Deng et al., 2011; Ortiz et al., 2011; Wang et al., 2013), optical spectroscopy (Allsop et al., 2013), impedance spectroscopy (Chen et al., 2013), fluorescence (Lin et al., 2012), surface enhanced Raman scattering (SERS) (Song et al., 2017), field-effect transistor (FET) (Chen et al.,

* Corresponding authors.
*E-mail addresses:* chiu@ntnu.edu.tw (H.-C. Chiu), cchan@mx.nthu.edu.tw (C.-C. Han), tjyen@mx.nthu.edu.tw (T.-J. Yen), hmchen@narlabs.org.tw (H.-M. Chen).
[1] Both D.-S. Su and P.-Y. Chen are the first authors.

https://doi.org/10.1016/j.bios.2019.03.042
Received 24 January 2019; Received in revised form 12 March 2019; Accepted 20 March 2019
Available online 21 March 2019
0956-5663/ © 2019 Elsevier B.V. All rights reserved.

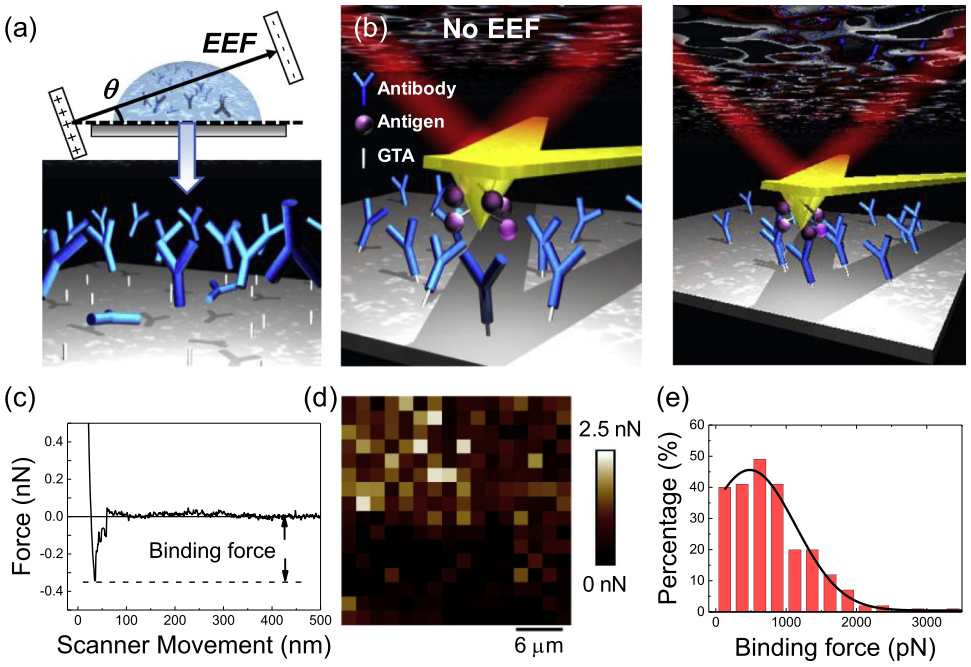


**Fig. 1.** External electric field with immobilization of proteins. (a) Experimental set-up of a rotational external electric field (EEF) applied to antibodies immobilized on a silicon chip surface. The angle (θ:0–360°)) of EEF is between substrate surface and the direction of EEF. (b) Cartoons showing the immobilization of antibodies without (left) and with (right) the optimal EEF. At its optimum, the polar antibodies are mostly reoriented in the right binding positions with antigens (pink balls). (c) Typical retracting curve of force vs. distance. Up-down arrows indicate the measured binding force. (d) Force-Volume mapping on a general chip coated by anti-CEACAM5 proteins. Brighter dots indicate larger binding forces. (e) Histogram showing all binding forces due to the results obtained from (d). Solid line indicates the best Gaussian fit. (For interpretation of the references to color in this figure legend, the reader is referred to the web version of this article).

2011; Cui et al., 2001) and carbon-nanotube-based biosensors (Yang et al., 2015) are also to have similar problems. However, these techniques may have a common strength to potentially replace ELISA due to their sensitivity, instant detection capability and cost-effectiveness *via* mass production. Especially, the field effect transistors (FET) *via* silicon nanowires (SiNWs) may be beneficial for the future application. Lieber's group[18] using SiNWs-FET to detect biological and chemical species is a pioneer in this approach.

Signal of SiNW-FET is due to the change in channel conductance and can be measured by the current change (ΔI). While, the measureable "ΔI" is always experienced too weak and unstable, especially for big biomolecules such as proteins. This problem may be explained due to the randomization effect of these proteins when they are immobilized on chip or other materials. For example, if the surface area of a nanowire can mostly afford for 10 antibody proteins (full occupied), but only less than 4 proteins are normally immobilized in the right position to be ready for binding with antigens (antibody proteins have their 3D dimension and only the right position of binding site can expose to correctly bind with their antigens). Therefore, the efficiency is less than 40%. If the criteria to reach the detectable level needs 8 proteins to be in right positions, the failed outcome is obtained. We experimented the current efficiency above is less than 30% (data not shown).

In this report, we try to partially solve the randomization problem above by using an external electric field (EEF). The purpose of EEF is to reorient these antibody proteins as they are immobilized on nanowires. For a demonstration, we use two cancer biomarkers, carcinoembryonic antigen (CEA)-related cell adhesion molecules 5 (CEACAM5) and 1 (CEACAM1) with their antibodies for the tests. Firstly, the optimal orientations of these antibodies in the general chip (6′) surface due to the binding forces measured by atomic force microscopy (AFM) are investigated under the influence of EEF ($_{max}EEF^{oa}$; oa means optimal angle). Secondly, these antibody proteins with the condition of $_{max}EEF^{oa}$s are immobilized in the nanowires and measured by EFT-ΔI. We certified that the binding efficiency between immobilized antibody and antigen is increased in the nanowires. The signals received are also stable. These results imply the possible application to the disease antigen detection in the future.

## 2. Experimental

### 2.1. Chemicals and reagents

CEACAM5, CEACAM1 and their antibodies are purchased from Merck Millipore (Burlington, MA, USA) without further purification. Glutaraldehyde (GTA) and [3- (2-Aminoethylamino)propyl]tri-methoxysilane (3-APTMS) are obtained from Sigma–Aldrich (St. Louis, MO, USA). AFM used is Bruker Multimode 8-HR. The electrical measurement system is CASCADE MICROTECH, summit 12000.

### 2.2. Sample preparation for AFM measurements

Before antibodies (anti-CEACAM5 and anti-CEACAM1) were immobilized on the silicon chip surfaces (~ 0.5 $cm^2$), several pretreatments were done: (a) the silicon substrates were cleaned by immersion in a piranha solution ($H_2SO_4$: $H_2O_2$ = 3:1) for 10 min (to remove all organic materials and impurities on the surface) and followed by oxygen plasma with 250 mTorr/80 W for 3 min (to create hydroxyl species on surface). (b) Treated silicon substrates were further immersed in 1% (v/v) ethanoic solution of 3-APTMS ((3-aminopropyl) trimethoxysilane) for 1 h (to establish a self-assembling monolayer (SAM) on the surface). (c) A cross-linker layer was formed by adding aqueous glutaraldehyde (GTA) and incubated for 30 min (to allow GTA covalently interacting with the SAM). Afterward, antibodies (50 μg/mL) in a phosphate-buffer (pH = 7.6) were then added into the treated silicon substrates for 30 min while EEF ($8 \times 10^5$ V/m) with different angles was also applied. As shown in Fig. 1(a), the angle between the applied electric field and the substrate surface was varied from 0° to 360°. If there has no EEF applied (Fig. 1(b), left figure), antibodies immobilized on chip surface may be random causing less binding possibilities with antigens. While, with optimal EEF° (Fig. 1(b), right figure), the re-oriented antibodies are in the right array positions causing high binding possibilities. In this experiment, we explore the optimal angle (oa) of EEF ($_{max}EEF^{oa}$)[20] for each anti-CEA antibody by investigating the AFM binding forces (see the next section) in a general chip. Afterward, the conditions of $_{max}EEF^{oa}$ were then used when the same antibodies were immobilized in the nanowires.

### 2.3. Antibody-antigen binding force measurements by AFM

Measurements of binding forces between antibody and antigen immobilized on a silicon ship surface were done by using a Bruker Multimode 8 AFM operated in the Force-Volume (FV) mapping mode. Spring constant was calibrated by thermal tune method (Hutter and Bechhoefer, 1993). During FV measurement, the AFM tip repeatedly approaches, contacts and retracts from the chip surface and the force *vs.* distance[22] was recorded (Fig. 1(c)). When the tip is in contact with the surface, antigens immobilized on the AFM's probe can bind well with antibodies immobilized on the chip if the binding sites of antibodies are in the appropriate positions. In other words, the AFM cantilever obtains a downward pulling force indicating the antigen-antibody binding strength. For each FV experiment, array of 16 × 16 force-distance curves through an area of 30 μm × 30 μm on the chip surface were acquired. Fig. 1(d) shows a typical FV binding force data array obtained from the investigation of anti-CEACAM5 immobilized on chip "without EEF". Under this condition, binding forces are not well distributed across the entire area indicating random orientation of antibodies on chip. Histogram of binding forces shown in Fig. 1(e) is based on the results from Fig. 1(d). A Gaussian fit was plotted and the majority of binding force (483 ± 51 pN in this case) was determined. At least 5 FV measurements were repeated on different surface locations.

### 2.4. Fabrication of silicon nanowires

The fabrication for producing nanowires was shown as below: (I) Silicon nanowires (SiNWs; n = 200 to 1000) were manufactured on a standard six-inch *p*-doped silicon wafer using "top-down" manner. Fabrication procedure with three I-line lithography processes was portrayed as shown in Fig. 2. (II) To fabricate the silicon nanowire (s) field effect transistor (SiNW-FET), a 70-nm-thick nitride on the silicon substrate (to produce a dielectric layer of FET) was done. Afterward, a 50-nm-thick polycrystalline silicon was completed and used as the conduction channel for charge carriers. (III) The first I-line lithography process was carried on a thin negative photoresist (PFI245) to construct nanowires on the substrate. The resolution of I-line lithography can be shrunk to one fifth of the feature size of a mask (Canon FPA-3000i5 + Stepper). For example, a line width of 400 nm can be achieved by I-line lithography using a mask that has a line width of 2 μm. Additionally, through the over-exposure of I-line lithography, the linewidth of a silicon nanowire can be narrowed down to 120 nm. The polycrystalline silicon was later etched by transformed coupled plasma (TCP poly etcher 9400) to pattern the nanowire structure. The dimensions of the obtained nanowires are typically ~120 nm in width and 30 μm in length. (IV) In order to activate the SiNW-FET, ion implantation using boron at a dose of $5 \times 10^5$ $cm^{-2}$ was carried out. During the ion implantation, a second I-line lithography process was performed to shield the nanowires. Post-annealing at 600 °C for 30 min by rapid thermal annealing (RTA) was then conducted (to reach a uniform distribution of boron layer in the doped area). (V) A third I-line lithography process was run (to define FET electrodes of S (source)/D (drain)). (VI) At the final stage, a 100 nm thick silicon oxide was deposited on top of the device, but exclude the region of nanowires and S/D electrodes. This procedure ensures most of antibodies will be grafted on the oxide-free silicon nanowire in later sample preparation because hydroxyl groups are more reactive on oxide-free silicon than silicon oxide (Thissen et al., 2012). In this work, number of nanowires from 200–1000 were produced and n = 1000 was used for the later experiments due to the results shown in Fig. 3. An image of scanning electron microscopy (SEM) for nanowires (n = 400) was shown in Fig. 3(a). The white dashed square indicates the location of fabricated nanowires in this device. Typical diameter of nanowires is around 121 nm. A multifunctional electrical measurement system (CASCADE MICROTECH, summit 12000 M) measuring the drain current changes (ΔI) after adding antigens into antibodies immobilized on nanowires was used. As shown in Fig. 3(b), Both drain and source voltages were tuned at 1 V and 0 V, respectively (Fig. 3(b)). Drain current ($I_D$) was measured by the condition of keeping gate current about 5% smaller than $I_D$ (to avoid gate current leakage). Fig. 3(c) shows results of the blank $I_{Ds}$ (without addition of proteins) obtained from different numbers of nanowires (n = 200–1000). At the same gate voltage (10V), the result shows that $I_D$ is increased with the number of nanowires (Fig. 3(d)). The error (standard deviation) is decreased from 8.4% (n = 200) to 4% (n = 1000). Accordingly, n = 1000 was selected for the later experiments.

## 3. Results and discussion

### 3.1. Optimization of the binding between antibody and antigen under an EEF in general chip

Since the binding force measurements of immobilized antibody using AFM cannot be done in the nanowires, a general chip (6′) is used first for searching $_{max}EEF^{oa}$. Both anti-CEACAM5 and anti-CEACAM1 immobilized on a chip were performed as EEF at different angles (0°, 45°, 90°, 135°, 180°, 225°, 270°, 315° and without EEF) were applied. Force volume (FV) of AFM was used to measure the binding forces between antigen and the immobilized antibody. FV images were shown in Fig. 4(a) and (b) for anti-CEACAM5/CEACAM5 and anti-CEACAM1/

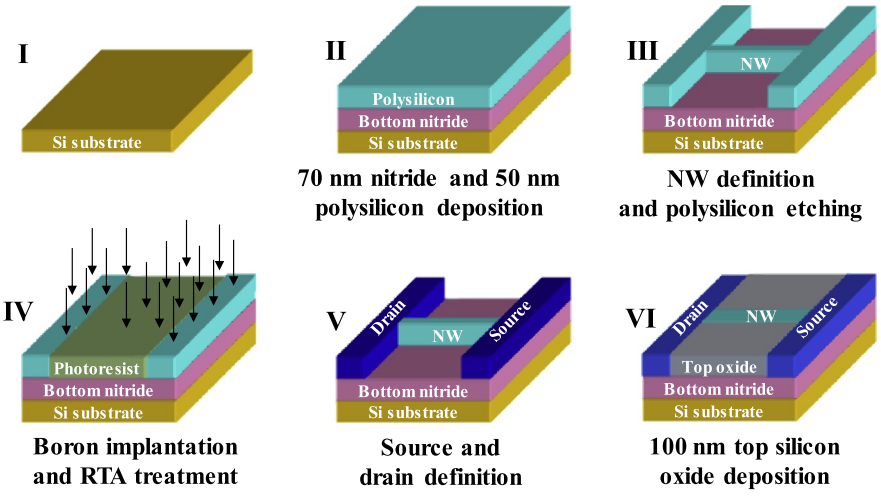


**Fig. 2.** Fabrication of SiNWs. Single nanowire (n = 1) is an example to show the key procedures from steps I to VI.

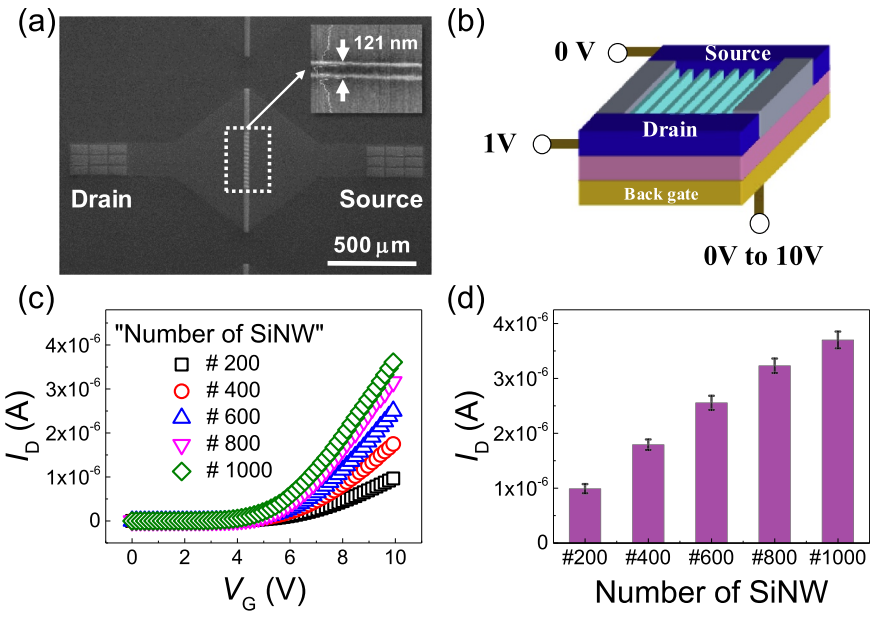


**Fig. 3. Nanowire investigations**. (a) Typical SEM image of SiNW-FET. The white dotted square indicates the location of SiNW channels. The insert shows a silicon nanowire that has a diameter of ~121 nm; (b) The measurement setup of SiNW-FET. During the measurements, the source and drain electrodes were kept at 0 V and 1 V, respectively, while the gate voltage $V_G$ changes from 0 V to 10 V to observe the change in drain current $I_D$; (c) The measured $I_D$ *vs.* $V_G$ from a SiNW-FET containing different number of nanowires (n = 200–1000); (d) The average $I_D$ vs. number of nanowires. 10 consecutive measurements were done.

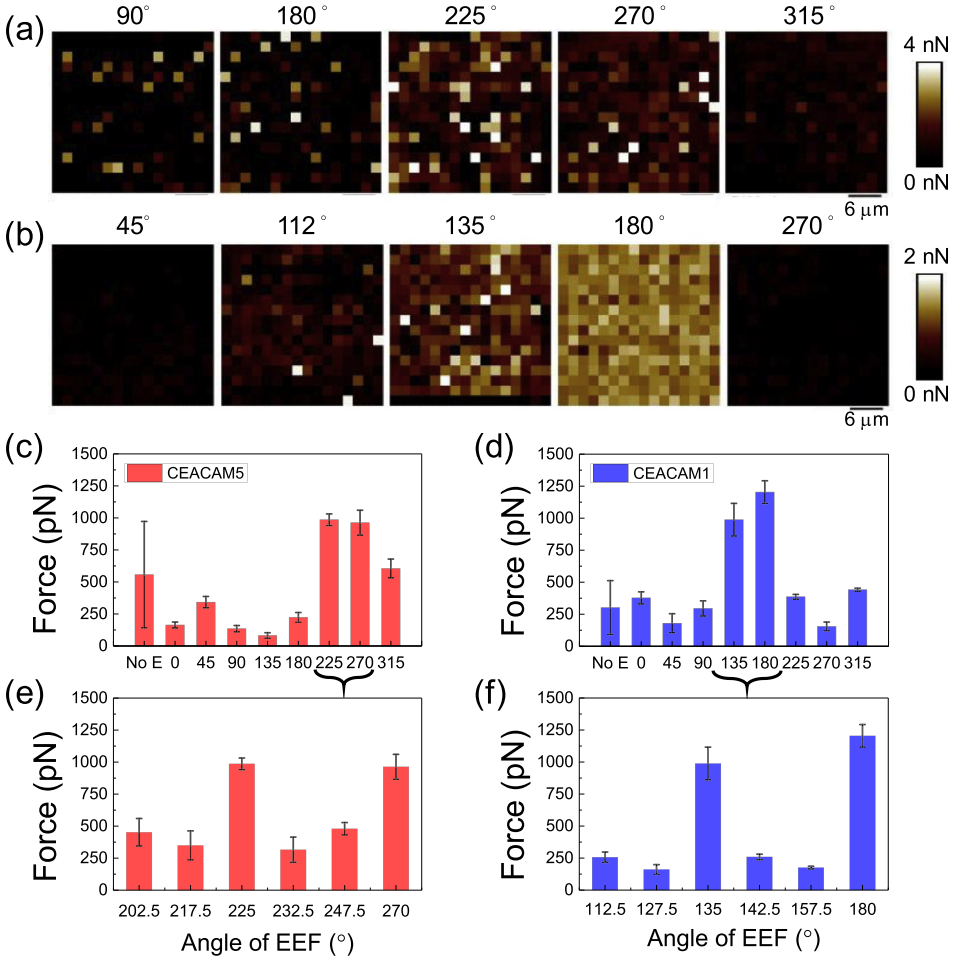


**Fig. 4.** AFM binding force measurements. Force volume maps at different angles of EEF were shown for anti-CEACAM5 (a) and anti-CEACAM1 (b), respectively. The calculated binding forces from these FV were shown in (c) and (d) for anti-CEACAM5 and anti-CEACAM1, respectively. More angels around the "maximum" (180°/270°) and (135°/180°) were selected for further tests for anti-CEACAM5/CEACAM5 (e) and anti-CEACAM1/CEACAM1 (f).

CEACAM1, respectively. The calculated binding forces were shown in Fig. 4(c) and (d). The maximum orientation of antibody proteins on chip at 225°/270° and 135°/180° for anti-CEACAM5 and anti-CEACAM1, respectively, were obtained. To further identify the "real maximum", more EEF's angles around 225° and 270° (202.5°, 217.5°, 225°, 232.5°, 247.5°, 270°) and around 135° and 180° (112.5°, 127.5°, 135°, 142.5°, 157.5°, 180°) were tested and results were shown in Fig. 4(e) and (d) for anti-CEACAM5/CEACAM5 and anti-CEACAM1/CEACAM1, respectively. Under these relatively detailed investigations, both $_{max}EEF^{oa}$s were obtained at $225^0$ ($_{max}EEF^{225}$) and $180^0$ ($_{max}EEF^{180}$) for anti-CEACAM5 and anti-CEACAM1, respectively (note: $_{max}$EEFs were found via trial and error. These may have an appropriate range around the maximum angles shown in this work). The efficiency (binding forces) with the optimal conditions (987 ± 45 pN for anti-CEACAM5 and 1205 ± 88 pN for anti-CEACAM1) were much larger as compared with those without EEF (558.1 ± 415.27 pN for anti-CEACAM5 and 303.27 ± 209.96 pN for anti-CEACAM1). The error is also bigger if EEF is not applied. The explanation is that proteins were randomized (or possible aggregated each other) when they get into the surface of a chip. Since most of proteins (especially antibodies) have their own charges forming a polar pole, the direction of the pole can be re-oriented only under the external forces such as electric field. Accordingly, the best re-orientation could be established only under the condition of $_{max}EEF^{oa}$ as shown in this report.

### 3.2. Antibody-antigen binding measurements under $_{max}EEF^{oa}$ in nanowires

The main purpose of this report is to demonstrate whether the measurements of antibody-antigen binding can be detected from sensitive tools such as nanowires. This is because nanowires having cost-effective pilot-scale production and high sensitivity can be possibly used in the future diagnostic market. With this concern, we applied the results of $_{max}EEF^{oa}$ obtained from general chip above to the nanowires. The fabrication of nanowires was shown in Fig. 2 and the total number of nanowires were made from n = 200 to n = 1000. Due to the results shown in Fig. 3, n = 1000 was selected for this section (SiNWs-EFT) tests: e.g., observations of ΔI change were done after antigen was added into the immobilized antibody on nanowires. A basic concept with the typical ΔI change was shown in Fig. 5(a). When antigen approaches to the antibody anchoring on the nanowires via their highly specific binding affinity, the surface of nanowires undergo a change in surface potential, resulting in a detectable drain current change, $\Delta I_D$, which is responsible for the change of the net charge from antigens. Since antigens were negatively charged, the change of surface potential on nanowires would cause accumulation of hole carriers in wire channels that lead to an increase of drain current[24] (positive $\Delta I_D$). In this experiment, $\Delta I_D$s at optimal and other angles of EEF were investigated after CEACAM5 (Fig. 5(b)) and CEACAM1 (Fig. 5(c)) were added into nanowire where their antibodies were immobilized on it. The results show that the $\Delta I_D$s were the largest at 2222.1 ± 206.4 nA and 963.3 ± 151.5 nA for anti-CEACAM5/CEACAM5 ($_{max}EEF^{225}$) and anti-CEACAM1/CEACAM1 ($_{max}EEF^{135}$), respectively. The second largest ones were at 1415.3 ± 398.3 nA and 900.8 ± 155.6 nA for anti-CEACAM5/CEACAM5 ($EEF^{270}$) and anti-CEACAM1/CEACAM1 ($EEF^{180}$), respectively. The outcomes above were about 10.8 times and 18.3 times as compared with those at $EEF^{90}$ and $EEF^{45}$ for anti-CEACAM5/CEACAM5, and about 30.8 times and 4.4 times at $EEF^{315}$ and $EEF^0$ for anti-CEACAM1/CEACAM1. There are two "largest" $\Delta I_{Ds}$ appearing at two angles of EEF: e.g., 225°/270° for anti-CEACAM5 and 135°/180° for anti-CEACAM1. Our explanation is that these antibodies have geographically two binding sites. Detailed experiments will be done in the near future for proving this issue.

In addition, the signal-to-noise ratio is substantially improved if the $_{max}EEF^{oa}$ is applied. For anti-CEACAM5, ratio is reduced from 20.6% (without EEF) to only 9.3% ($_{max}EEF^{225}$). For anti-CEACAM1, it is reduced from 43.8% (without EEF) to 15.7% ($_{max}EEF^{135}$). These results clearly indicate that accuracy of the antigens' detection with nanowires as tool can be achieved by the application of $_{max}EEF^{oa}$.

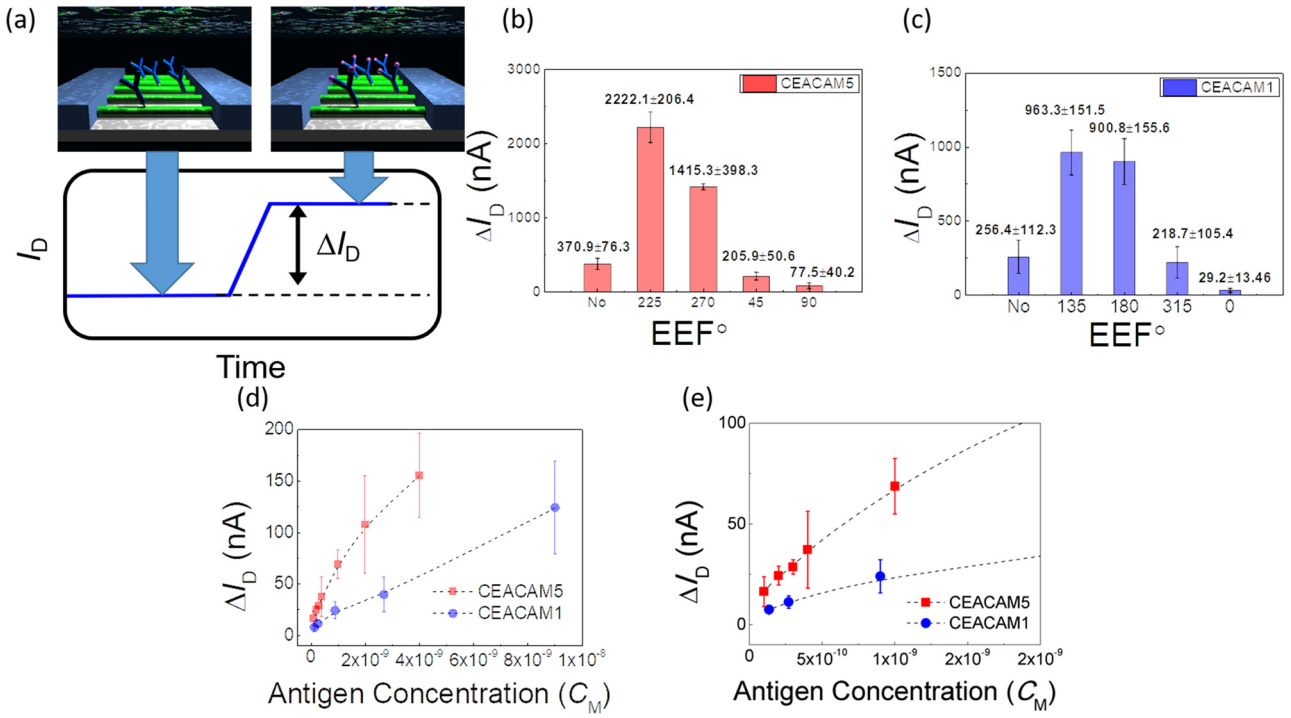


**Fig. 5. Measurements of the current change in nanowires.** (a) Schematic view of drain current change ($\Delta I_D$) due to antigen (pink dots) and antibody (Y-type) bindings on nanowires; (b)& (c) $\Delta I_D$ measurements of SiNWs-EFT (n = 1000) at $_{max}EEF^{oa}$ (225° and 180°) and other angles of EEF for anti-CEACAM5/CEACAM5 and anti-CEACAM1/CEACAM1, respectively. All binding forces were indicated at various angles of EEF; (d)& (e) $\Delta I_D$ versus concentration of antigen. The detection limits of SiNWs-FET are around 18 ng/mL and 21.6 ng/mL for CEACAM5 and CEACAM1, respectively. (For interpretation of the references to color in this figure legend, the reader is referred to the web version of this article).

To determine the detection limit of the current nanowire system, both stock concentration of antigens (50 μg/mL, or $2.2 \times 10^{-7}$ M and $2.5 \times 10^{-7}$ M for CEACAM5 (MW: 180 kD) and CEACAM1 (MW:160 kD), respectively) were constantly diluted and each dilution of $\Delta I_D$ was measured. The minimum $\Delta I_D$ that can be detectable in the current experimental setup is about 16.5 ± 7.3 nA and 7.5 ± 1.4 nA for CEACAM5 and CEACAM1, respectively, which corresponds to the antigen concentrations of $1.0 \times 100^{-10}$ M (18 ng/mL) and $1.35 \times 10^{-10}$ M (21.6 ng/mL), respectively (Fig. 5(d) and (e)). Further study and improvement will be done to reach less than 10 ng/mL for clinical diagnostics[16,25] in the future. The method shown in this report is innovative. There has an interesting article (Song, et. al., 2017) similarly describing the detection of the cancer antigen (cancer carcinoembryonic antigen; CEA) by using Raman spectroscopy. However, the following two points may be outstanding from our works: (i) We use a novel EEF technique to optimize the immobilization of antibodies on chip causing the efficiency and cost-effective used later for the commercial applications. (ii) We use semiconductor/nanowires by measuring the current change directly (without adding additional materials). While, to obtain Raman signals reported by Song et. al., one needs an additional compound, RhodG tagged aptamer.

## 4. Conclusion

Protein antibodies can be efficiently reoriented on a chip under the influence of an external electric field (EEF) and the optimal angle of EEF ($_{max}EEF^{oa}$) can be obtained by atomic force microscopy. Further use of $_{max}EEF^{oa}$ to the nanowires for detecting cancer antigens has been approved. Studies of more sensitive and stable nanowires with more effective EEF may be done for the clinical applications in the future.

## Acknowledgements

This work was supported by grant from the Ministry of Science and Technology, Taiwan (MOST-103-2221-E-492-032 from H.-M. Chen). We appreciated the supports of nanowires and fabrication from National Applied Research Laboratories/Taiwan Semiconductor Research Institute.

## Declaration of interests

The authors declare that they have no known competing financial interests or personal relationships that could have appeared to influence the work reported in this paper.

## References

Al-Shereiqi, A.S., Boyd, B.J., Saito, K., 2015. Photo-responsive self-assemblies based on bio-inspired DNA-base containing bolaamphiphiles. Chem. Commun. 51 (25), 5460–5462.

Allsop, T., Neal, R., Dvorak, M., Kalli, K., Rozhin, A., Webb, D.J., 2013. Physical characteristics of localized surface plasmons resulting from nano-scale structured multilayer thin films deposited on D-shaped optical fiber. Opt. Express 21 (16), 18765–18776.

Bracha, D., Karzbrun, E., Daube, S.S., Bar-Ziv, R.H., 2014. Emergent properties of dense DNA phases toward artificial biosystems on a surface. Acc. Chem. Res. 47 (6), 1912–1921.

Caruso, F., Rodda, E., Furlong, D.N., Niikura, K., Okahata, Y., 1997. Quartz crystal microbalance study of DNA immobilization and hybridization for nucleic Acid sensor development. Anal. Chem. 69 (11), 2043–2049.

Chen, K.-I., Li, B.-R., Chen, Y.-T., 2011. Silicon nanowire field-effect transistor-based biosensors for biomedical diagnosis and cellular recording investigation. Nano Today 6 (2), 131–154.

Chen, Z., Huang, Y., Li, X., Zhou, T., Ma, H., Qiang, H., Liu, Y., 2013. Colorimetric detection of potassium ions using aptamer-functionalized gold nanoparticles. Anal. Chim. Acta 787, 189–192.

Cui, Y., Wei, Q., Park, H., Lieber, C.M., 2001. Nanowire nanosensors for highly sensitive and selective detection of biological and chemical species. Science 293 (5533), 1289–1292.

Deng, L., Norberg, O., Uppalapati, S., Yan, M., Ramstrom, O., 2011. Stereoselective synthesis of light-activatable perfluorophenylazide-conjugated carbohydrates for glycoarray fabrication and evaluation of structural effects on protein binding by SPR imaging. Org. Biomol. Chem. 9 (9), 3188–3198.

Dong, G.-C., Chuang, P.-H., Forrest, M.D., Lin, Y.-C., Chen, H.M., 2006. Immuno-suppressive effect of blocking the CD28 signaling pathway in T-cells by an active component of echinacea found by a novel pharmaceutical screening method. J. Med. Chem. 49 (6), 1845–1854.

Han, S.M., Cho, J.H., Cho, I.H., Paek, E.H., Oh, H.B., Kim, B.S., Ryu, C., Lee, K., Kim, Y.K., Paek, S.H., 2007. Plastic enzyme-linked immunosorbent assays (ELISA)-on-a-chip biosensor for botulinum neurotoxin A. Anal. Chim. Acta 587 (1), 1–8.

Hutter, J.L., Bechhoefer, J., 1993. Calibration of atomic-force microscope tips. Rev. Sci. Instrum. 64 (7), 1868–1873.

Lin, Z., Zhang, G., Yang, W., Qiu, B., Chen, G., 2012. CEA fluorescence biosensor based on the FRET between polymer dots and Au nanoparticles. Chem. Commun. 48 (79), 9918–9920.

Ortiz, M., Fragoso, A., O'Sullivan, C.K., 2011. Amperometric detection of antibodies in serum: performance of self-assembled cyclodextrin/cellulose polymer interfaces as antigen carriers. Org. Biomol. Chem. 9 (13), 4770–4773.

Rusmini, F., Zhong, Z., Feijen, J., 2007. Protein immobilization strategies for protein biochips. Biomacromolecules 8 (6), 1775–1789.

Seo, S.M., Cho, I.H., Jeon, J.W., Cho, H.K., Oh, E.G., Yu, H.S., Shin, S.B., Lee, H.J., Paek, S.H., 2010. An ELISA-on-a-chip biosensor system coupled with immunomagnetic separation for the detection of vibrio parahaemolyticus within a single working day. J. Food Prot. 73 (8), 1466–1473.

Sin, M.L.Y., Mach, K., Wong, P.-.K., Liao, J., 2014. Advances and challenges in biosensor-based diagnosis of infectious diseases.

Song, G., Zhou, H., Gu, J., Liu, Q., Zhang, W., Su, H., Su, Y., Yao, Q., Zhang, D., 2017. Tumor marker detection using surface enhanced Raman spectroscopy on 3D Au butterfly wings. J. Mater. Chem. B 5 (8), 1594–1600.

Thissen, P., Peixoto, T., Longo, R.C., Peng, W., Schmidt, W.G., Cho, K., Chabal, Y.J., 2012. Activation of surface hydroxyl groups by modification of H-terminated Si (111) surfaces. J. Am. Chem. Soc. 134 (21), 8869–8874.

Wang, R., Du, L., Zhang, C., Man, Z., Wang, Y., Wei, S., Min, C., Zhu, S., Yuan, X.C., 2013. Plasmonic petal-shaped beam for microscopic phase-sensitive SPR biosensor with ultrahigh sensitivity. Opt. Lett. 38 (22), 4770–4773.

Xing, J.Z., Zhu, L., Jackson, J.A., Gabos, S., Sun, X.-J., Wang, X.-b., Xu, X., 2005. Dynamic monitoring of cytotoxicity on microelectronic sensors. Chem. Res. Toxicol. 18 (2), 154–161.

Yang, N., Chen, X., Ren, T., Zhang, P., Yang, D., 2015. Carbon nanotube based biosensors. Sens. Actuators B: Chem. 207, 690–715.